

# Multiscale Simulations of Material with Heterogeneous Structures Based on Representative Volume Element Techniques

Zeliang Liu<sup>1</sup>, C. T Wu<sup>1</sup>, Bo Ren<sup>1</sup>, Wing Kam Liu<sup>2</sup>, Roger Grimes<sup>1</sup>

<sup>1</sup> Livermore Software Technology Corporation, Livermore, CA 94551

<sup>2</sup> Northwestern University, Evanston, IL 60208

## Abstract

*This paper presents a concurrent multiscale simulation framework for materials with heterogeneous structures (e.g. composite). This avoids the burdens of finding the macroscale phenomenological models and tedious calibration processes by directly establishing the connection between the microstructure and macro-response through computational homogenization. In the homogenization process, the model links every macroscopic integration point to a Representative Volume Element (RVE) of the microstructure, and macroscopic response is obtained by solving the RVE boundary value problem. Direct numerical simulation (DNS) techniques (e.g. FEM) for RVE analysis are capable of providing accurate high-fidelity material response data for complex phase morphology and behavior. Meanwhile, it is necessary to accelerate the RVE analysis using advanced model reduction techniques to enable efficient concurrent simulations.*

*RVE analysis package based on the FEM implicit analysis has been developed for 2D and 3D problems. Both smp and mpp are enabled. Instead of using separated pre- and post-processing packages for other FEA software, we have integrated the whole RVE analysis processes into LS-DYNA<sup>®</sup>, including preparing boundary conditions, FE analysis of the boundary value problem and RVE homogenization. Some key features of the RVE analysis package are 1) automatically assign boundary conditions to a given RVE mesh, such as periodic BC and uniform BC; 2) non-matching meshes on the faces can be considered; 3) arbitrary loading directions, such as uniaxial and shear; 4) output the RVE homogenization results to LS-DYNA database, for both small-strain and finite-strain problem.*

*All the above functions are now covered by two new keywords in LS-DYNA, \*RVE\_ANALYSIS\_FEM and \*DATABASE\_RVE. Some numerical benchmarks will be utilized to demonstrate the capability of the RVE package. The linkage of the RVE package and the development of data-driven model reduction techniques will also be discussed.*

## 1. Introduction

Materials are hierarchical in nature; hence, they involve an inter-play between simple small-scale constituents that together form elaborate compounds that can span multiple time- and length-scales. On the other hand, advanced manufacturing techniques, such as 3D printing [1-3], allow us to make hierarchically structured composites from nano- to macro-scale, which exhibit advantageous thermal, electrical or mechanical properties [4]. This multi-scale nature of heterogeneous materials poses a continuing challenge in computational modeling of macroscopic structures. Ideally, efficient and accurate predictions of the macroscopic behavior of heterogeneous materials should be uniquely obtained from the material behavior of each separate constituent (material phase) and from the information about the material microstructure [5].

Traditional phenomenological constitutive relations [6-8] characterize the average behaviors of the material, i.e. the contributions from all the material phases are not accounted for as an individual interaction of separate constituents. These laws regard materials as "black boxes", implying the need for burdensome experimental characterization and tedious calibration. In addition, they are problem-dependent and tend to fail when capturing highly localized microstructure-induced nonlinear material behavior, such as plasticity, damage and fatigue. Generalized continuum mechanics, also known as higher-gradient theories, have been proposed to

incorporate the microscopic information by introducing higher order gradient of deformation [9]. The first known generation is micromorphic continuum developed by Toupin [10], Mindlin [11] and Eringen [12], and it is further generalized with arbitrary number of extra strain gradients by Liu and co-workers [13]. A current challenge of high-gradient theories is the determination of the large number of coefficients associated with higher-order tensors [14]. The strain gradient is usually not directly informed by the microstructure, making the model phenomenological and requiring extra effort to calibrate those coefficients.

Concurrent multiscale methods [15,16] avoid the calibration process in the phenomenological models by directly establishing the connection between the microstructure and the macro-response of materials using the so-called homogenization method. In the homogenization process, these concurrent methods link every macroscopic point of a structure to a Representative Volume Element (RVE) of the microstructure, and the macroscopic response (e.g. stress) is obtained through averaging inside the RVE. For a material with random microstructure, its true macroscopic properties are obtained as converged values only if the size of the RVE becomes sufficiently large, or the RVE should be a statistically representative sample of the material. Based on the DNS RVE analysis using FEA or FFT-methods, model reduction techniques can be then applied to accelerate the concurrent simulations. Figure 1 shows an example of concurrent simulation using a data-driven method called self-consistent clustering analysis (SCA) [17,18].

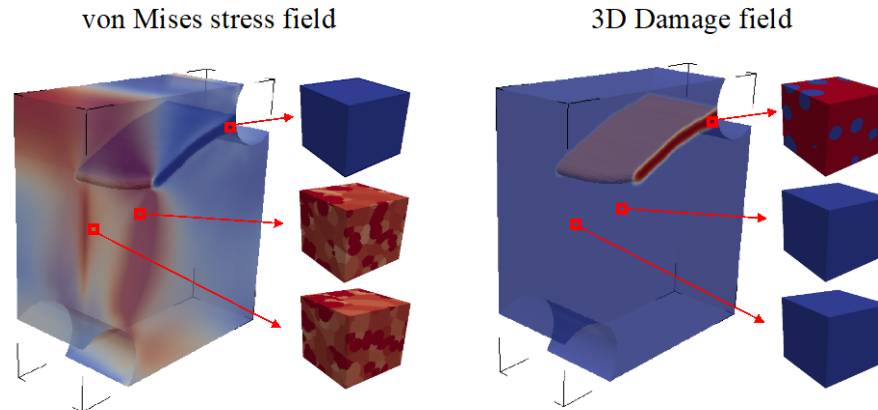


Figure 1 Illustration of a concurrent multiscale simulation based on RVE analysis and data-driven methods. The macroscopic material responses are driven by microscale RVE boundary value problem. The RVE package introduced in the paper will serve as the basis for the concurrent simulation.

In this paper, the recent developed RVE package in LS-DYNA will be presented. In Section 2, the general homogenization theory is discussed, including the definition of an RVE. Different choices of the boundary conditions and the treatment of non-matching meshes are presented in Section 3. All the functions of the RVE package are covered by two new keywords in LS-DYNA, `*RVE_ANALYSIS_FEM` and `*DATABASE_RVE`, which are introduced in Section 4. In Section 5, the RVE package are validated by several numerical examples. Based on the RVE-analysis package, a large amount of RVE response data can be generated for training our data-driven material models, using machine learning techniques. The on-going research regarding this topic will be briefly discussed in Section 6.

## 2. Homogenization theory

First-order homogenization, which will be mainly used in this dissertation, can be defined by assuming scale-separation and vanishing external body force inside the RVE. Let us introduce  $\mathcal{U}$  as the space of admissible microscopic displacements  $\mathbf{u}$  inside an RVE domain  $\Omega$  with boundary  $\Gamma$ . It can be proved that under classical first-order boundary conditions, such as displacement boundary conditions (DBC), traction boundary condition (TBC) and periodic boundary conditions (PBC), the following equation is satisfied under small strain assumption,

$$\langle \boldsymbol{\sigma} \rangle_{\Omega} : \langle \delta \boldsymbol{\varepsilon} \rangle_{\Omega} = \langle \boldsymbol{\sigma} : \delta \boldsymbol{\varepsilon} \rangle_{\Omega}, \quad \forall \delta \mathbf{u} \in \mathcal{U} \quad (1)$$

where  $\boldsymbol{\sigma}$  and  $\boldsymbol{\varepsilon}$  are the Cauchy stress and infinitesimal strain, respectively. Moreover,  $\langle \dots \rangle_{\Omega}$  is defined as volume average inside the RVE,

$$\langle \dots \rangle_{\Omega} = \frac{1}{\Omega} \int_{\Omega} \dots d\Omega \quad (2)$$

Eq. (1) is the so-called Hill-Mandel macro-homogeneity condition [19,20], which is equivalent to the statement that the virtual work density on the macroscale equals that of the microscale. It also ensures that the homogenized strain and stress are admissible variables in the macroscale constitutive relation.

For finite strain problem, the Hill-Mandel condition can be rewritten as

$$\langle \mathbf{P} \rangle_{\Omega} : \langle \delta \mathbf{F} \rangle_{\Omega} = \langle \mathbf{P} : \delta \mathbf{F} \rangle_{\Omega}, \quad \forall \delta \mathbf{u} \in \mathcal{U} \quad (3)$$

The finite strain formulation is more general and can be degenerated to Eq (1) under small strain assumption. As a result, the current RVE package uses the finite strain formulation with the deformation gradient  $\mathbf{F}$  and first Piola-Kirchhoff stress  $\mathbf{P}$  as the strain and stress measures.

In terms of the size of RVE, it should be large enough so that sufficient statistical microstructural information of the material can be included. Theoretically, it is always beneficial to have a larger RVE in order to obtain accurate homogenization results. However, in practice, the RVE size cannot be too large due to the limit of computational cost. The best way to determine the appropriate RVE size is to do a convergence study and select the smallest size that satisfies the tolerance (e.g. 5%).

Direct Numerical Simulation (DNS) is the most accurate and flexible homogenization method for solving the RVE problem, e.g. Finite Element Method and Fast Fourier Transformation (FFT)-based micromechanics method [21]. The current RVE package developed in LS-DYNA is based on FEM, due to its flexibility of treating complex geometries and non-uniform mesh. If the RVE has a large number of degrees of freedom, DNS can be very time-consuming. The time issue can be more serious in a concurrent multiscale simulation, since each integration point is associated with a RVE model. Thus, it is necessary to use model reduction techniques to accelerate the RVE analysis. Some on-going research topics of developing new machine learning techniques to enable fast and accurate multiscale simulations will be discussed in Section 6.

### 3. RVE boundary conditions

Given the macroscopic constraints of stress or strain, different types of boundary conditions can be prescribed on the RVE. Currently, the periodic boundary conditions and displacement boundary conditions have been implemented in LS-DYNA. The illustrations of these two types of boundary conditions are shown in Figure 2 under uniaxial tension loading. It has been demonstrated in the literature that the periodic BC needs a smaller RVE size to get converged RVE homogenization results, and the displacement BC usually yields a stiffer response since all the faces are forced to be flat as shown in the figure. However, if the RVE size is large enough, the influence of the BC type is trivial.

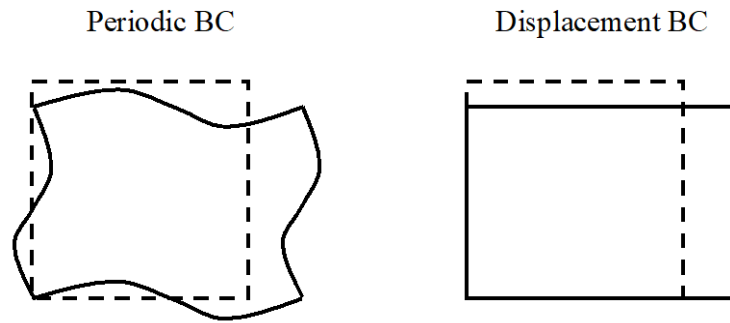


Figure 2 Illustrations of periodic and displacement BCs with the same macroscopic strain constraint on the RVE.

For both periodic and displacement BCs, the macroscopic strain constraint on the RVE is prescribed through the so-called control points, which are additional points to the original RVE model. In a 2D problem, there are in total two control points, while there are three control points for a 3D problem. The relationships between the displacement of control points and macroscopic strain is shown in the figure below.

		$u_x$	$u_y$	
2D problem	$c^1$	$(\bar{F}_{xx} - 1)\Delta x$	$\bar{F}_{yx}\Delta x$	
	$c^2$	$\bar{F}_{xy}\Delta y$	$(\bar{F}_{yy} - 1)\Delta y$	
3D problem		$u_x$	$u_y$	$u_z$
	$c^1$	$(\bar{F}_{xx} - 1)\Delta x$	$\bar{F}_{yx}\Delta x$	$\bar{F}_{zx}\Delta x$
	$c^2$	$\bar{F}_{xy}\Delta y$	$(\bar{F}_{yy} - 1)\Delta y$	$\bar{F}_{zy}\Delta y$
	$c^3$	$\bar{F}_{xz}\Delta z$	$\bar{F}_{yz}\Delta z$	$(\bar{F}_{zz} - 1)\Delta z$

$c$ : control point;  $u$ : displacement;  $\bar{F}$ : deformation gradient

Figure 3 The relationship between displacements of the control nodes and macroscopic deformation gradient in both 2D and 3D

When the deformation gradients of the RVE are not fully constrained in the shear direction, the solution is not unique and would cause numerical problems. Thus, additional constraints are provided for the off-diagonal components (shown for a general 3D case),

$$\bar{F}_{yx} = \bar{F}_{xy}, \quad \bar{F}_{zx} = \bar{F}_{xz}, \quad \bar{F}_{yz} = \bar{F}_{zy}, \quad (4)$$

which indicates that the averaged deformation gradient is symmetric. In terms of the displacement components, we have

$$u_y^{c^1} \Delta y = u_x^{c^2} \Delta x, \quad u_z^{c^1} \Delta z = u_x^{c^3} \Delta x, \quad u_z^{c^2} \Delta z = u_y^{c^3} \Delta y, \quad (5)$$

where  $(\Delta x, \Delta y, \Delta z)$  represent the dimensions of the RVE. Note that it is not necessary that all the dimensions should be the same. For an arbitrary RVE mesh, the dimensions will be automatically measured by the program and stored for related calculations.

The RVE boundary value program is solved using the implicit solver in LS-DYNA. After the FE analysis, the RVE needs to be homogenized to get the macroscopic material responses. Instead of taking the volume averaging based on Eq. (1) and (3), a more efficient way is to directly extract the macroscopic quantities on the control points. The relationship between the reaction forces on the control points and macroscopic stress is shown in the figure below.

		$f_x$	$f_y$	
2D problem	$c^1$	$\bar{P}_{xx}\Delta y\Delta z$	0	
	$c^2$	$2\bar{P}_{xy}\Delta x\Delta z$	$\bar{P}_{yy}\Delta x\Delta z$	
		$f_x$	$f_y$	$f_z$
3D problem	$c^1$	$\bar{P}_{xx}\Delta y\Delta z$	0	0
	$c^2$	$2\bar{P}_{xy}\Delta x\Delta z$	$\bar{P}_{yy}\Delta x\Delta z$	0
	$c^3$	$2\bar{P}_{xz}\Delta x\Delta y$	$2\bar{P}_{yz}\Delta x\Delta y$	$\bar{P}_{zz}\Delta x\Delta y$

$c$ : control point;  $f$ : reaction force;  $\bar{P}$ : first Piola-Kirchhoff stress

Figure 4 The relationship between reaction force of the control nodes and macroscopic first Piola-Kirchhoff stress in both 2D and 3D

Under the constraints in Eq. (4), the first Piola-Kirchhoff stress is also symmetric,

$$\bar{P}_{yx} = \bar{P}_{xy}, \quad \bar{P}_{zx} = \bar{P}_{xz}, \quad \bar{P}_{zy} = \bar{P}_{yz}, \quad (6)$$

Once the homogenized deformation gradient and first Piola-Kirchhoff stress are determined, other strain and stress measures (e.g. infinitesimal strain and Cauchy stress) can be easily calculated. All the macroscopic quantities will automatically be collected by the program and output to the database per users' request.

For displacement boundary conditions, a vertex of the RVE is chosen as the origin and fixed to remove rigid body motion. The displacement of a node on the faces  $\mathbf{u}$  with coordinate  $\mathbf{X} = \{x, y, z\}$  is constraint by

$$\mathbf{u} = \bar{\mathbf{F}} \cdot \mathbf{X} \quad (7)$$

The situation of periodic boundary condition is more complex. For a pair of nodes  $\{\mathbf{u}^1, \mathbf{u}^2\}$  on the x-y plane, the following constrain equations need to be satisfied,

$$u_x^2 - u_x^1 = u_x^{c1}, \quad u_y^2 - u_y^1 = u_y^{c1}, \quad u_z^2 - u_z^1 = u_z^{c1} \quad (8)$$

Similarly, the constraint equations for nodes on the y-z and x-z planes can also be derived. Moreover, a node inside the RVE is fixed to get rid of rigid body motion.

Non-matching mesh problem for periodic boundary condition are solved by the concept of master and slave faces. For each pair of faces, the one with less number of nodes is chosen as the master face, and the other one becomes the slave face. As shown in Figure 5, the nodes (denoted by  $i, j, k$ ) on the slave face are projected to the master surface. The projected nodes are then constrained by the nodes on the master face. For example, if

the projected node  $j'$  of node  $j$  falls into the element with nodes  $I, J, K$ , the displacement of node  $j'$  is constrained by

$$\mathbf{u}^{j'} = \mathbf{N}^I \mathbf{u}^I + \mathbf{N}^J \mathbf{u}^J + \mathbf{N}^K \mathbf{u}^K, \tag{9}$$

where  $\mathbf{N}^I$  is the element shape function of node  $I$  at the position of node  $j'$ .

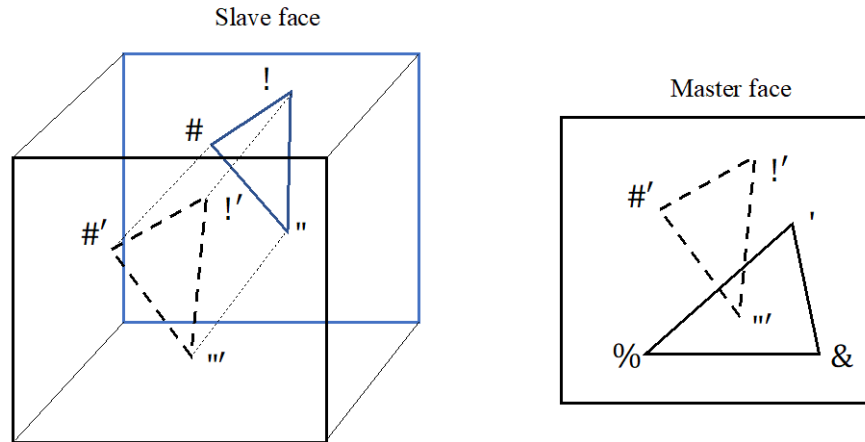


Figure 5 Treatment of non-matching meshes

The method based on master and slave faces still have issues of unbalanced force and may affect the accuracy of the prediction. Therefore, if possible, a matching RVE mesh is always preferred. However, when it is hard or impossible to obtain a good matching mesh, this method based on slave and master faces can be utilized to apply the periodic boundary conditions.

#### 4. LS-DYNA keywords for RVE analysis

The RVE package can be accessed through two new keywords in the LS-DYNA, “\*RVE\_ANALYSIS\_FEM” and “\*DATABASE\_RVE. In this section, we will introduce these two keywords in detail.

“\*RVE\_ANALYSIS\_FEM” is the main keyword for the RVE analysis, and its input options are provided in Figure 6.

Card 1	1	2	3	4	5	6	7	8
Variable	MESHFILE							
Type	A80							
Default	None							

Card 1	1	2	3	4	5	6	7	8
Variable	MESHFILE							
Type	A80							
Default	None							

Card 3	1	2	3	4	5	6	7	8
Variable	E11	E22	E33	E23	E13	E12		
Type	F	F	F	F	F	F		
Default	None	None	None	None	None	None		

Figure 6 Input options for keyword \*RVE\_ANALYSIS\_FEM

“MESHFILE” is the name of the user input file which contains the mesh info of the RVE. “INPT” identifies whether the boundary condition file is given by the user. If not (INPT=0), the program will generate a new file named “RVE\_MESHFILE” which includes the input for the boundary conditions. “LCID” is loading curve id specified by the keyword “\*DEFINE\_CURVE”. “IDOF” is the RVE dimension (2 or 3). “BC” identifies the type of boundary condition. Currently, the package support periodic boundary conditions (BC=0) and displacement boundary conditions (BC=1). “IUNI” tells the program whether the given RVE has a matching mesh (IUNI=1). Note that the algorithm of generating periodic BC is more efficient for IUNI=1. The input options in Card 3 are the components of strain prescribed on the RVE,

$$E_{ii} = F_{ii} - 1, \quad E_{ij} = F_{ij} (i \neq j) \quad (10)$$

If the input for a strain component is empty, stress-free condition will be applied in that direction. For 2D problems (IDOF=2), inputs for E33, E23, E13 are ignored.

“\*DATABASE\_RVE” is keyword for the output of the RVE analysis. The input options are shown in Figure 7.

Card 1	1	2	3	4	5	6	7	8
Variable	DT	BINA						
Type	F	I						
Default	None	0						

Figure 7 Input options for keyword \*DATABASE\_RVE

“DT” stands for the time interval of database output. “BINA” determine whether the program will output the homogenization results to a ASCII database file named “rveout” (BINA=0) or to the LS-DYNA binary database (BINA=1).

## 5. Numerical examples

Several numerical examples are presented to validate the capability of the RVE package in both 2D (plane strain) and 3D. First, 2D and 3D RVEs with inclusions embedded in the matrix are investigated under finite deformation. Both matrix and inclusion materials are chosen to be isotopically hypoelastic. The elastic material constants are  $E_{matrix} = 100MPa$ ,  $E_{inclusion} = 1GPa$  and  $\nu_{matrix} = 0.3$ ,  $\nu_{inclusion} = 0.3$ . The results under periodic and displacement BCs are provided in Figure 8.

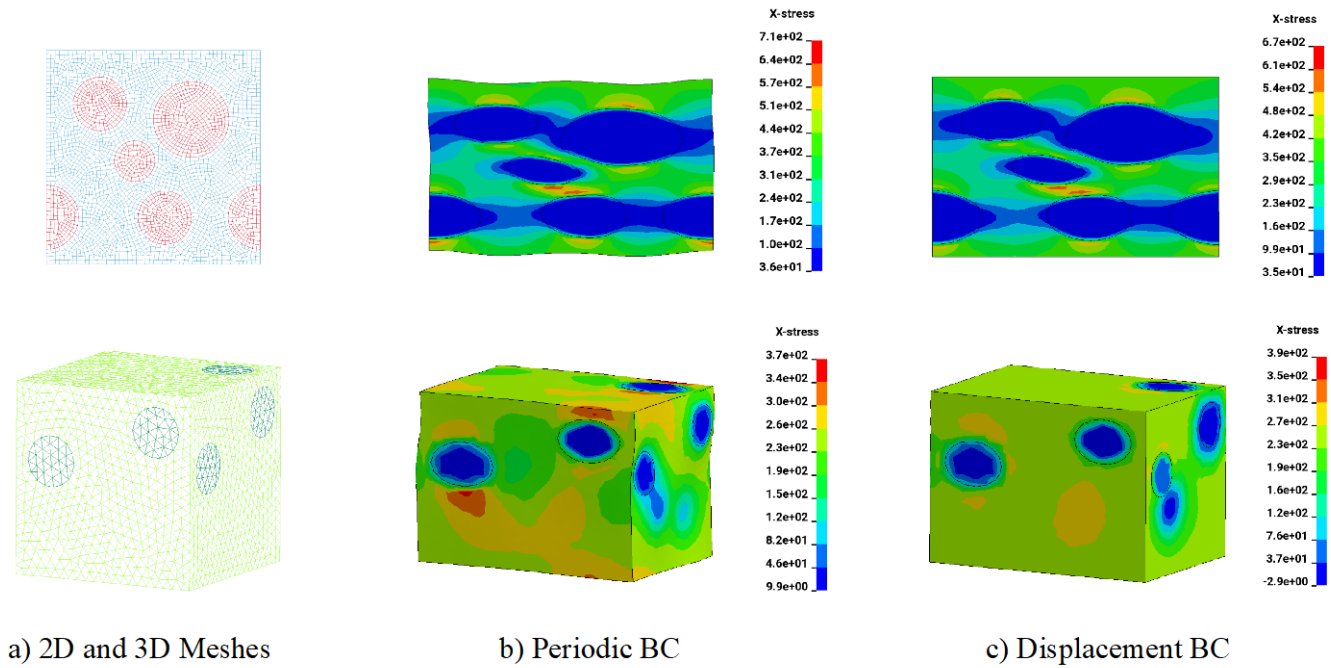


Figure 8 RVE analysis results under uniaxial tension ( $E_{11} = 0.4$ ) for periodic and displacement BCs.

With the control points, we can easily prescribe various loading conditions on the RVE. Figure 9 shows the 3D simulation results under uniaxial tension, shear and mixed loadings.

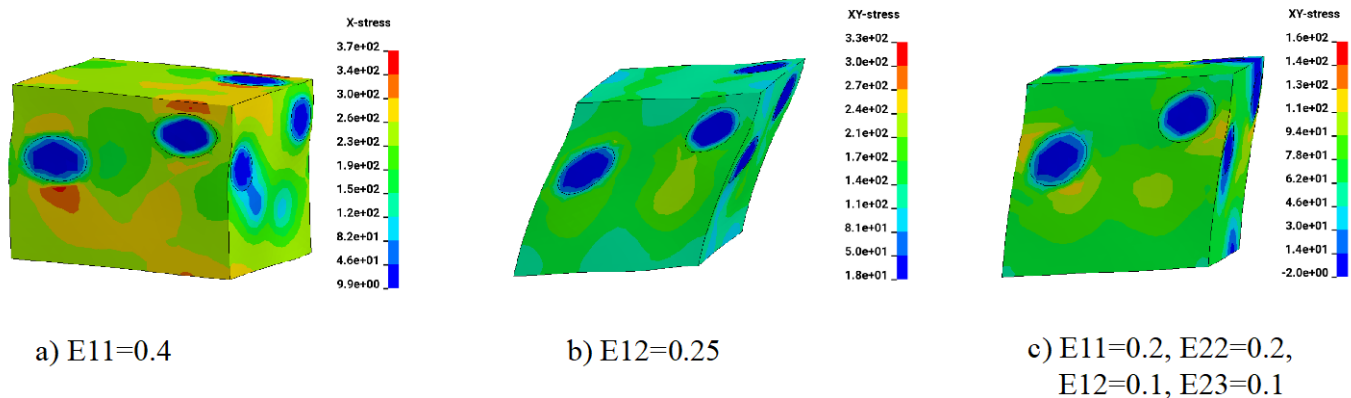


Figure 9 Simulation results under uniaxial, shear and mixed loading conditions

Finally, the RVE package is used to simulate carbon fiber reinforced woven composite. The matrix material is chosen to be isotropic elastic, with material constant  $E_{matrix} = 3GPa$  and  $\nu_{matrix} = 0.2$ . The yarn can be considered as a composite with unidirectional fiber embedded in the matrix material, so the yarn material is assumed to be orthotropic elastic. The properties of the yarn in the fiber directions are  $E_a = 200GPa, E_b = 10GPa, E_c = 10GPa, \nu_{ba} = 0.02, \nu_{ca} = 0.02, \nu_{cb} = 0.4, G_{ab} = 5GPa, G_{bc} = 5GPa, G_{ca} = 5GPa$ . Periodic BC is applied on the RVE. The simulation results under uniaxial tension ( $E_{11}=0.01$ ) are shown in Figure 10.

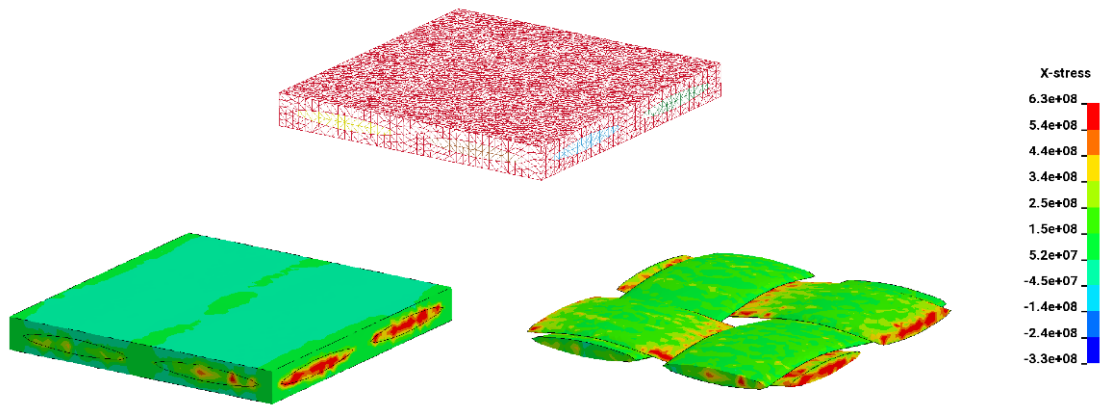


Figure 10 Simulation results of woven composites under uniaxial tension  $E_{11}=0.01$ .

## 6. On-going research on data-driven material modeling

The modelling complexity from the interaction between the microstructures in the microscale propagates to the macroscale, and it becomes challenging to describe the macroscale behavior using a closed-form phenomenological constitutive law. The new RVE package in LS-DYNA is a good tool for generating high-fidelity macroscopic material property data from microstructural information. However, in order to conduct a multiscale concurrent simulation, the RVE analysis relies on DNS is still very time consuming. Thus, one of our on-going research topics is on data-driven material modeling and exploring new ways of constructing multiscale material database. It will be a combination of mechanistic homogenization theory and machine learning approach based on a large number of data generated from RVE analysis.

Meanwhile, current machine learning techniques (e.g. deep learning) has achieved great successes in broad areas of computer engineering, such as computer vision, gaming, and natural language processing. Although these techniques are able to construct models for complex input-output relations, their applications to mechanics of materials are still limited. Issues like material history dependency and physical invariance are not naturally resolved, mainly due to the loss of physics in the current learning models. The difficulty of finding the responses of a heterogeneous material becomes apparent when material nonlinearity (e.g. hyperelastic, plasticity, damage) and arbitrary loading path are considered. Now we are studying on new mechanistic machine learning models with less loss of physics for RVE property predictions. It is also possible to adopt similar models to other areas of computational mechanics where information transmission across scales is important, such as manufacturing and crash simulations.

## References

- [1] Jakus, A. E., Secor, E. B., Rutz, A. L., Jordan, S. W., Hersam, M. C., and Shah, R. N. Three-dimensional printing of high-content graphene scaffolds for electronic and biomedical applications. *ACS nano* 9, 4(2015), 4636–4648.
- [2] Meza, L. R., Das, S., and Greer, J. R. Strong, lightweight, and recoverable three-dimensional ceramic nanolattices. *Science* 345, 6202 (2014), 1322–1326.
- [3] Meza, L. R., Zelhofer, A. J., Clarke, N., Mateos, A. J., Kochmann, D. M., and Greer, J. R. Resilient 3D hierarchical architected metamaterials. *Proceedings of the National Academy of Sciences of the United States of America* 112, 37 (2015), 11502–7.
- [4] Ramanathan, T., Abdala, A., Stankovich, S., Dikin, D., HerreraAlonso, M., Piner, R., Adamson, D., Schniepp, H., Chen, X., Ruoff, R., et al. Functionalized graphene sheets for polymer nanocomposites. *Nature nanotechnology* 3, 6 (2008), 327–331.
- [5] Z. Liu, Reduced-order Homogenization of Heterogeneous Material Systems: from Viscoelasticity to Nonlinear Elasto-plastic

- Softening Material. PhD Thesis (2017).
- [6] Gurson, A. L. Continuum theory of ductile rupture by void nucleation and growth: Part i—yield criteria and flow rules for porous ductile media. *Journal of engineering materials and technology* 99, 1 (1977), 2–15.
- [7] de Souza Neto, E., Peric, D., and Owen, D. *Computational methods for plasticity: theory and applications*. Wiley, 2008.
- [8] Werner, B. T., and Daniel, I. M. Characterization and modeling of polymeric matrix under multi-axial static and dynamic loading. *Composites Science and Technology* 102 (2014), 113–119.
- [9] Geers, M. G., Kouznetsova, V. G., and Brekelmans, W. Multi-scale computational homogenization: Trends and challenges. *Journal of computational and applied mathematics* 234, 7 (2010), 2175–2182.
- [10] Mindlin, R. D. Micro-structure in linear elasticity. *Archive for Rational Mechanics and Analysis* 16, 1 (1964), 51–78.
- [11] Toupin, R. A. Theories of elasticity with couple-stress. *Archive for Rational Mechanics and Analysis* 17, 2 (1964), 85–112.
- [12] Eringen, A. C. Mechanics of micromorphic continua. In *Mechanics of generalized continua*. Springer, 1968, pp. 18–35.
- [13] Vernerey, F., Liu, W. K., and Moran, B. Multi-scale micromorphic theory for hierarchical materials. *Journal of the Mechanics and Physics of Solids* 55, 12 (2007), 2603–2651.
- [14] Tran, T.-H., Monchiet, V., and Bonnet, G. A micromechanics-based approach for the derivation of constitutive elastic coefficients of strain-gradient media. *International Journal of Solids and Structures* 49, 5 (2012), 783–792.
- [15] Feyel, F., and Chaboche, J.-L. Fe 2 multiscale approach for modelling the elastoviscoplastic behaviour of long fibre sic/ti composite materials. *Computer methods in applied mechanics and engineering* 183, 3 (2000), 309–330.
- [16] Kouznetsova, V., Geers, M. G. D., and Brekelmans, W. A. M. Multiscale constitutive modelling of heterogeneous materials with a gradient-enhanced computational homogenization scheme. *International Journal for Numerical Methods in Engineering* 54, 8 (2002), 1235–1260.
- [17] Z. Liu, M.A. Bessa, and W.K. Liu. Self-consistent clustering analysis: an efficient multi-scale scheme for inelastic heterogeneous materials. *Computer Methods in Applied Mechanics and Engineering* 306 (2016): 319-341.
- [18] Z. Liu, M. Fleming, and W.K. Liu. Microstructural material database for self-consistent clustering analysis of elastoplastic strain softening materials." *Computer Methods in Applied Mechanics and Engineering* (2017).
- [19] Hill, R. Elastic properties of reinforced solids: some theoretical principles. *Journal of the Mechanics and Physics of Solids* 11, 5 (1963), 357–372.
- [20] Hill, R. A self-consistent mechanics of composite materials. *Journal of the Mechanics and Physics of Solids* 13, 4 (1965), 213–222
- [21] Moulinec, H., and Suquet, P. A numerical method for computing the overall response of nonlinear composites with complex microstructure. *Computer methods in applied mechanics and engineering* 157, 1 (1998), 69–94.